Molecular Crystals and Liquid Crystals
Publication details, including instructions for authors and subscription information:
http://www.tandfonline.com/loi/gmcl16

Studies on Mesogenic Disc-like Molecules III. Heat Capacity of Benzene-hexa-n-octanoate from 13 to 393 K

Michio Sorai [a], Hideki Yoshioka [a] & Hiroshi Suga [a]
[a] Chemical Thermodynamics Laboratory, Department of Chemistry, Faculty of Science, Osaka University, Toyonaka, Osaka, 560, Japan
Version of record first published: 14 Oct 2011.

To cite this article: Michio Sorai , Hideki Yoshioka & Hiroshi Suga (1982): Studies on Mesogenic Disc-like Molecules III. Heat Capacity of Benzene-hexa-n-octanoate from 13 to 393 K, Molecular Crystals and Liquid Crystals, 84:1, 39-54

To link to this article: http://dx.doi.org/10.1080/00268948208072130

Mol. Cryst. Liq. Cryst., 1982, Vol. 84, pp. 39–54
0026-8941/82/8401-0039 $06.50/0

Printed in the United States of America

Studies on Mesogenic Disc-like Molecules III. Heat Capacity of Benzene-hexa-*n*-octanoate from 13 to 393 K†

MICHIO SORAI, HIDEKI YOSHIOKA and HIROSHI SUGA

Chemical Thermodynamics Laboratory and Department of Chemistry, Faculty of Science, Osaka University, Toyonaka, Osaka 560, Japan

(*Received May 25, 1981; in final form September 9, 1981*)

The heat capacity of benzene-hexa-*n*-octanoate, $C_6(OCOC_7H_{15})_6$, with a purity of 99.77 mole per cent has been measured with an adiabatic-type calorimeter in the range from 13 to 393 K. Three phase transitions were found at 301.89 (Phase II → I), 355.10 (Phase I → columnar mesophase) and 357.09 K (columnar mesophase → isotropic liquid). The enthalpy and entropy of these transitions were 48.96 kJ mol^{-1}/164.01 J K^{-1} mol^{-1}, 46.07/129.81 and 19.22/53.77, respectively. The infrared spectra recorded in the range 4000-30 cm^{-1} showed a drastic change between the two crystalline phases. The spectra of the mesophase were substantially the same as those of the isotropic liquid. As in the case of $C_6(OCOC_6H_{13})_6$, the heat capacity of the mesophase was much smaller than those of the adjacent crystalline and isotropic liquid phases. This compound also acquired a large amount of transition entropy due to conformational melting of the paraffinic moieties in the solid state. The flexible paraffinic moieties play an important role for the appearance of the columnar mesophase.

1 INTRODUCTION

When a new mesophase formed by disc-like molecules came on the state in 1977,[1] this was thought to be an unusual condensed state of matter contradicting the accepted image of classical rod-like liquid crystals in various aspects. In fact diverse experimental facts accumulated after that have clearly supported that this is an entirely new type of liquid crystal, quite unlike the classi-

† Contribution No. 22 from Chemical Thermodynamics Laboratory. Part II of this series is Ref. 16.

cal nematic or smectic types. From a structural point of view, many of disc-like molecules, though not all, are stacked in columns and the different columns form hexagonal or rectangular lattice in the mesophase.[1-9] And hence this new type of mesophase has been described as discotic,[10] canonic[6,11] or columnar.[11,12]

Based on thermodynamic and infrared absorption studies on the disc-like molecules of a homologous series of benzene-hexa-*n*-alkanoate,[1,2] we found that these compounds exhibit solid-to-solid phase transitions accompanied by a large amount of transition entropy due to conformational melting of the paraffinic moieties.[13-16] In consequence, the melting entropy was a small portion of the cumulative transition entropy. In the case of the discotic mesogen, $C_6(OCOC_6H_{13})_6$, the melting entropy was only 1.5 times as much of the transition entropy at clearing point.[14-16] Moreover, the heat capacity of this compound was much smaller in the columnar mesophase than in the adjacent crystalline and isotropic liquid phases: quite unlike the classical nematic or smetic phases.

The present paper has been aimed to confirm these characteristics by measuring heat capacity and infrared spectrum of benzene-hexa-*n*-octanoate, $C_6(OCOC_7H_{15})_6$, over a wide temperature region.

2 EXPERIMENTAL

The compound was synthesized from inositol and *n*-caprylyl chloride in accordance with the published methods.[17-19] The product was recrystallized four times from absolute ethanol and dried for 30 h in a vacuum. *Anal.* Calcd. for $C_{54}H_{90}O_{12}$: C, 69.64%; H, 9.74%. Found: C, 69.58%; H, 9.69%.

The heat capacities were measured with an adiabatic-type calorimeter[20] in the range from 13 to 393 K. A calorimeter cell[21] made of gold and platinum contained 17.6875 g (≙ 0.0189923 mol) of the compound and a small amount of helium gas to aid the heat transfer.

The infrared spectra in the range 4000-30 cm^{-1} were recorded for Nujol mulls between 96 and 368 K. Optical textures of the crystalline and mesophases were observed by a polarizing microscope equipped with a heating stage. The models of the infrared spectrophotometers and the microscope have been described previously.[13,16]

3 RESULTS

The results of the calorimetric measurements were evaluated in terms of C_p, the molar heat capacity under a constant pressure. The experimental data are listed in Table I and plotted in Figure 1. In addition to the melting at 355.10 K and the mesophase-to-isotropic liquid transition at 357.09 K having been pre-

TABLE I

Molar heat capacity of $C_6(OCOC_7H_{15})_6$: Relative molecular mass 931.298

T/K	C_p/J K^{-1} mol^{-1}	T/K	C_p/J K^{-1} mol^{-1}	T/K	C_p/J K^{-1} mol^{-1}
12.431	18.172	164.027	846.52	324.319	2120.5
13.633	24.364	168.183	861.15	326.047	2116.8
14.845	31.021	172.324	876.77	330.243	2104.3
16.027	37.766	176.445	892.12	331.850	2100.7
17.163	44.402	180.554	907.64	335.966	2094.6
18.292	51.386	184.652	923.78	340.085	2090.2
19.503	59.403	188.740	939.60	344.202	2090.3
20.812	67.879	192.833	955.69	348.309	2102.1
22.574	81.063	196.934	971.84	350.983	2119.6
24.671	96.760	200.343	986.28	351.239	2133.4
26.722	112.77	204.430	1002.5	352.211	2178.4
28.965	130.91	208.512	1019.4	353.401	2343.9
31.245	149.38	212.600	1036.9	354.362	4282.7
33.324	166.39	216.702	1055.4	354.817	26758.
35.494	184.42	221.221	1075.7	354.928	60113.
37.875	203.94	225.676	1091.4	354.983	99252.
40.269	223.04	229.673	1111.4	355.018	155020.
42.662	241.89	233.626	1132.1	355.041	221210.
45.049	259.94	237.586	1153.6	355.058	300840.
47.694	279.47	241.572	1175.6	355.070	382660.
50.570	300.66	245.540	1195.9	355.080	473300.
53.372	321.82	249.513	1222.1	355.089	501570.
56.635	345.62	253.504	1247.7	355.100	344900.
59.797	368.82	256.837	1270.1	355.193	13784.
63.086	390.45	260.228	1294.5	355.688	1912.0
66.734	413.92	263.599	1322.2	356.405	2959.2
70.552	437.89	267.605	1356.3	356.808	12502.
74.158	459.04	271.569	1394.5	356.941	33974.
77.593	478.92	275.487	1436.1	357.000	59723.
80.567	495.29	279.346	1485.8	357.036	85840.
83.052	508.85	280.864	1499.6	357.063	111420.
86.303	526.21	283.138	1544.0	357.085	128250.
89.662	543.33	286.855	1615.4	357.107	110780.
93.071	560.37	289.603	1678.6	357.439	2817.8
96.368	576.28	291.397	1734.3	358.389	2167.2
100.371	594.60	293.151	1800.9	361.094	2156.7
104.431	612.96	295.303	1895.3	364.968	2139.2
108.416	630.75	296.966	2010.7	369.144	2124.6
112.354	647.09	298.559	2173.0	373.334	2112.4
116.345	663.80	300.021	2421.3	377.534	2103.5
120.385	680.80	301.234	3790.9	381.738	2095.7
124.428	696.69	301.815	75377.	385.944	2091.2
128.451	712.60	301.891	173070.	390.147	2087.1
132.492	728.39	301.954	124080.		
135.857	741.48	302.221	20388.		
139.897	756.36	303.714	2883.9	Undercooled Phase I	
143.986	772.40	306.704	2221.8		
148.118	785.67	309.779	2199.2	308.474	2166.1
152.251	802.26	313.689	2170.2	312.309	2156.6
155.694	815.39	317.728	2148.6	316.258	2144.7
159.861	830.82	321.866	2129.3	320.268	2132.0

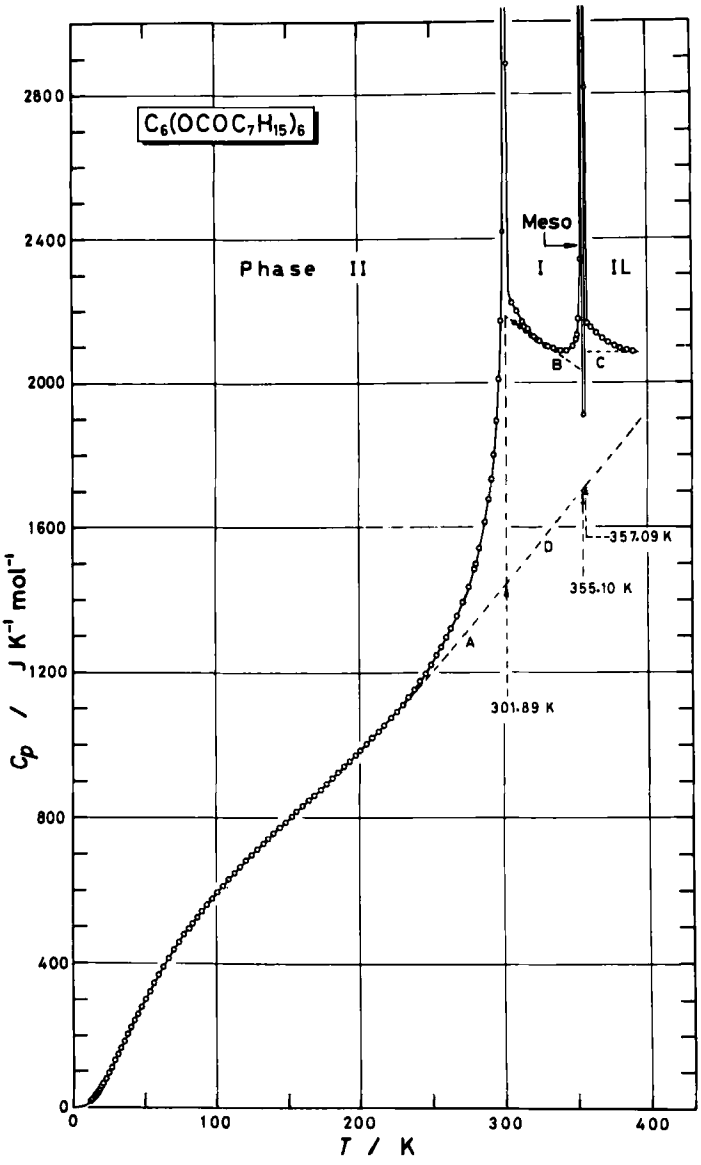

FIGURE 1 Molar heat capacity of $C_6(OCOC_7H_{15})_6$. The columnar mesophase and isotropic liquid phase are abbreviated as "Meso" and "IL", respectively. The solid circles in Phase I represent the data of the undercooled Phase I. The broken lines labelled A, B and C correspond to the estimated normal heat capacities for Phases II and I, and the isotropic liquid phase.

viously reported,[1,2] a new solid-to-solid phase transition was found at 301.89 K. All these transitions were characteristic of a first-order. The high- and low-temperature crystalline phases will be hereafter denoted as Phases I and II.

The time required for thermal equilibration after an energy input was usually 20 min or shorter, while it was elongated to one hour or longer in the vicinity of these three phase transition points. Since the temperature interval in which the mesophase exists stably is quite narrow, i.e., 1.99 K (= 357.09 − 355.10), only one successful measurement of the heat capacity of this phase was made at 355.688 K. The heat capacity of 1912.0 J K^{-1} mol^{-1} at this point seems to represent the "true" value characteristic of the mesophase because the thermal equilibration times at the initial (355.280 K) and final (356.097 K) temperatures of this run were quite short; say, shorter than 20 min in contrast to much longer temperature-drifts of the adjacent runs (1.5 h or longer).

The purity of the sample was determined by a fractional fusion method. Plot of the reciprocal of the fraction melted against the melting temperature gave a straight line, indicating nonexistence of solid-soluble impurities, and the slope yielded a sample purity of 99.77 mole per cent. The triple point of pure material was 355.154 K.

The standard thermodynamic functions of $C_6(OCOC_7H_{15})_6$ were calculated from the heat capacity data and the calorimetric enthalpy measurements across the respective phase transitions. Table II contains a listing of values for the heat capacity, C_p°, the entropy, S°, the enthalpy function, $(H^\circ - H_0^\circ)/T$, and the Gibbs energy function, $-(G^\circ - H_0^\circ)/T$, at selected temperatures. The values in parentheses were derived from an effective frequency spectrum, the estimation of which will be described in Section 4.

The infrared absorption spectra recorded at various phases are reproduced in Figures 2, 3 and 4. Owing to the narrow temperature interval of the mesophase, it was difficult to keep the temperature of the sample in this range during a long scanning time of the far-infrared spectroscopy. Hence, the spectrum of the mesophase has not been given in Figure 4.

The transitions could be seen very clearly by a polarizing microscope equipped with a heating stage. When the sample was cooled from the isotropic liquid to the mesophase, a broken fan-shaped texture appeared (Figure 5(a)). Though not frequently, a variant of the focal conic texture with spherulitic domains was also observed (Figure 5(b)). On going from the mesophase to Phase I, the optical view changed to paramorphic mosaic texture and simultaneously a contraction of the molar volume induced to generate cracks (Figure 5(c)). On further cooling, a change in the texture was observed at the transition from Phase I to Phase II (Figure 5(d)).

4 DISCUSSION

As shown in Figure 1, the heat capacity of the highest-temperature solid phase (Phase I) of the present compound was decreased with increasing tempera-

TABLE II

Standard thermodynamic functions for $C_6(OCOC_7H_{15})_6$ in J K^{-1} mol^{-1}

T/K	C_p°	S°	$(H^\circ - H_0^\circ)/T$	$-(G^\circ - H_0^\circ)/T$
5	(1.26)	(0.421)	(0.316)	(0.105)
10	(10.03)	(3.364)	(2.522)	(0.842)
20	62.62	24.315	17.898	6.417
30	139.30	63.762	45.235	18.527
40	220.89	115.08	79.083	35.995
50	296.46	172.61	115.14	57.471
60	370.16	233.23	151.60	81.631
70	434.42	295.17	187.49	107.68
80	492.17	357.02	221.96	135.06
90	545.02	418.09	254.98	163.11
100	592.90	478.04	286.49	191.55
120	679.18	593.91	344.87	249.04
140	756.76	704.50	398.23	306.27
160	831.35	810.40	447.69	362.71
180	905.55	912.58	494.42	418.16
200	984.83	1012.0	539.45	472.60
220	1070.2	1109.8	583.72	526.09
240	1166.9	1206.8	627.96	578.81
260	1292.9	1312.7	673.99	638.73
280	1491.7	1407.3	724.72	682.61
298.15	2131.3	1514.3	784.43	729.87
	Phase transition (II → I) at 301.89 K			
320	2138.0	1792.9	997.17	795.76
340	2090.3	1920.7	1062.5	858.20
	Phase transition (I → Mesophase) at 355.10 K			
	Phase transition (Mesophase → Liquid) at 357.09 K			
360	2160.9	2219.0	1296.2	922.80
380	2098.9	2333.9	1339.8	994.09
390	2087.3	2388.2	1359.1	1029.12

ture; in contrast to the homologous compounds with shorter paraffinic moieties, for which the heat capacity was an increasing function of temperature.[13-16] We at first thought that this might be caused by the post-transitional effect of the solid-to-solid phase transition at 301.89 K. However, since the heat capacity of the undercooled Phase I (the solid circles in Figure 1) also showed a similar tendency, this turned out to be an intrinsic character of Phase I, and thus the post-transitional effect was very small. A possible origin responsible for the decrease in the heat capacity of Phase I may arise from excitations in rotational-vibration modes of the paraffinic moieties. One-dimensional rotator is known to exhibit its heat capacity maximum of the order of the gas constant, R, in the temperature region where the thermal energy is comparable with its potential barrier, while the heat capacity approaches to $R/2$ in the limit of free-rotator.[22] In fact, as shown in Figures 2, 3 and 4, the infrared spectra clearly indicate random and rapid molecular motions in Phase I. A number of well-resolved absorption bands have been recorded in Phase II, whereas the

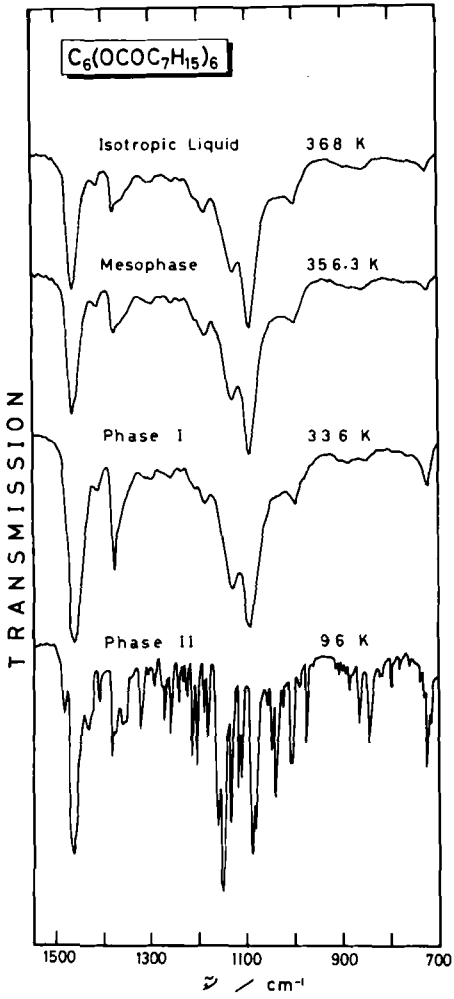

FIGURE 2 Infrared spectra of $C_6(OCOC_7H_{15})_6$.

number of bands has been extremely reduced and the bands become broader and more smeared in Phase I. This fact suggests that the molecular motions are suppressed in Phase II and molecules are arranged in an ordered state, while in Phase I the paraffinic moieties move rapidly and randomly, and thus the averaged site-symmetries become high.

In a previous paper[16] we found that the heat capacity of the columnar mesophase of $C_6(OCOC_6H_{13})_6$ is much smaller than those of the adjacent crystalline and isotropic liquid phases. This situation is also encountered for the present compound (see Figure 1). Although the available C_p point in the mesophase is only one, the heat capacity is really much smaller than those of the

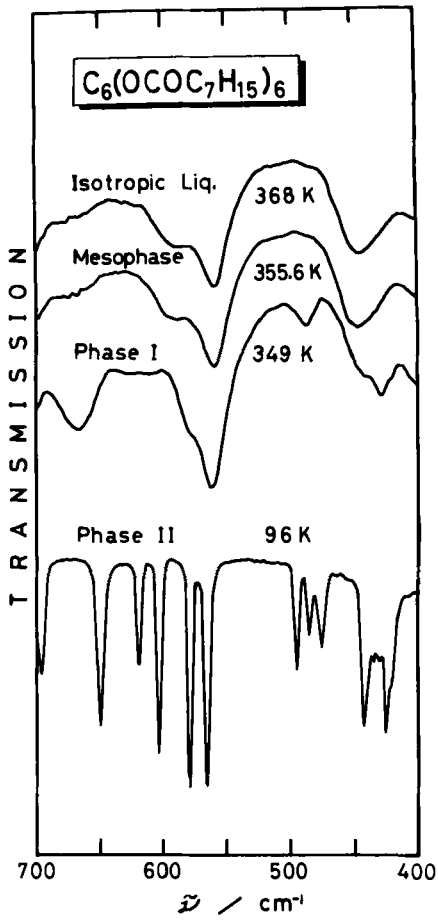

FIGURE 3 Infrared spectra of $C_6(OCOC_7H_{15})_6$.

adjacent phases. We can, therefore, regard the small heat capacity as being one of the characteristic features inherent in the columnar mesophase.

Another remarkable feature of the discotic mesogen is a short-range order effect still persisting in the isotropic liquid state, which appears as the heat capacity tail above the clearing point (Figure 1). This type of short-range order was also observed for a discotic mesogen, $C_6(OCOC_6H_{13})_6$,[16] while in contrast to this a non-discotic homologue, $C_6(OCOC_5H_{11})_6$, did not show such an effect.[13] This effect may be interpreted by assuming the existence of clusters consisting of a partial columnar arrangement in the isotropic liquid state.

To separate the excess heat capacities due to the phase transitions from the experimental values, appropriate "normal" heat capacities were estimated by

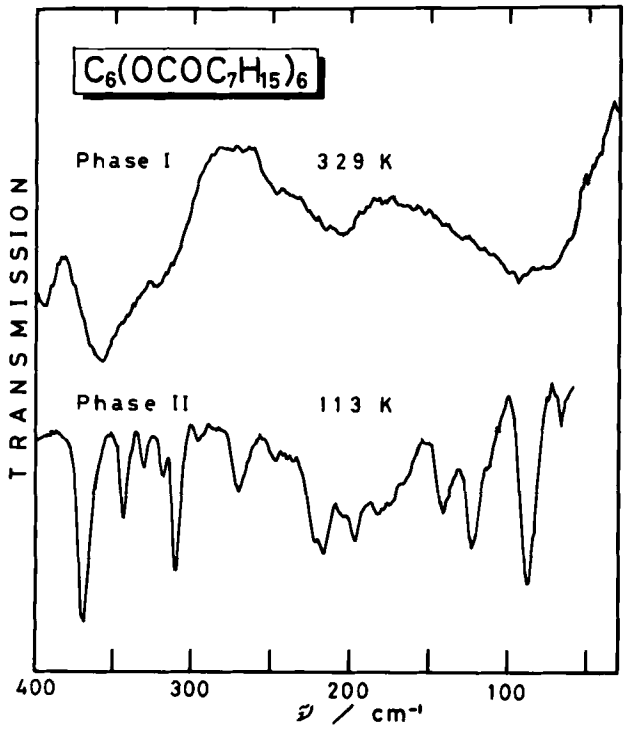

FIGURE 4 Far-infrared spectra of $C_6(OCOC_7H_{15})_6$.

an effective frequency spectrum method.[23] The normal heat capacity for Phase II was determined by using 60 C_p values between 12.4 and 196.9 K and the vibrational frequencies of 37 "modes" (426 degrees of freedom) obtained from the infrared spectra in the range from 2950 to 700 cm^{-1}. A "best" fit was obtained for a continuous spectrum consisting of two Debye-type and three constant distributions; $G(\tilde{\nu}) = 0.1394 \times 10^{-3}\tilde{\nu}^2$ (0 − 80 cm^{-1}), $G(\tilde{\nu}) = 0.3520 \times 10^{-4}\tilde{\nu}^2$ (80 − 150 cm^{-1}), $G(\tilde{\nu}) = 0.2839$ (150 − 333 cm^{-1}), $G(\tilde{\nu}) = 0.6700 \times 10^{-1}$(333 − 517 cm^{-1}) and $G(\tilde{\nu}) = 0.8351 \times 10^{-1}$(517 − 700 cm^{-1}). The effective spectrum thus obtained was able to reproduce the experimental C_p values in this temperature region within ±0.567 J K^{-1} mol^{-1}. The normal heat capacities for Phase II calculated from this spectrum is shown by the broken line (A) in Figure 1. The broken curve (D) above 301.89 K corresponds to the heat capacities due to this spectrum. The normal heat capacity of Phase I (the broken line (B)) was simply regarded as being represented by a straight line connecting the experimental heat capacity data of the undercooled Phase I. In the isotropic liquid phase, a straight line passing through the highest-temperature C_p point at 390.147 K and parallel to the axis of abscissas (the broken line (C)) was regarded as the normal heat capacity. Finally for the

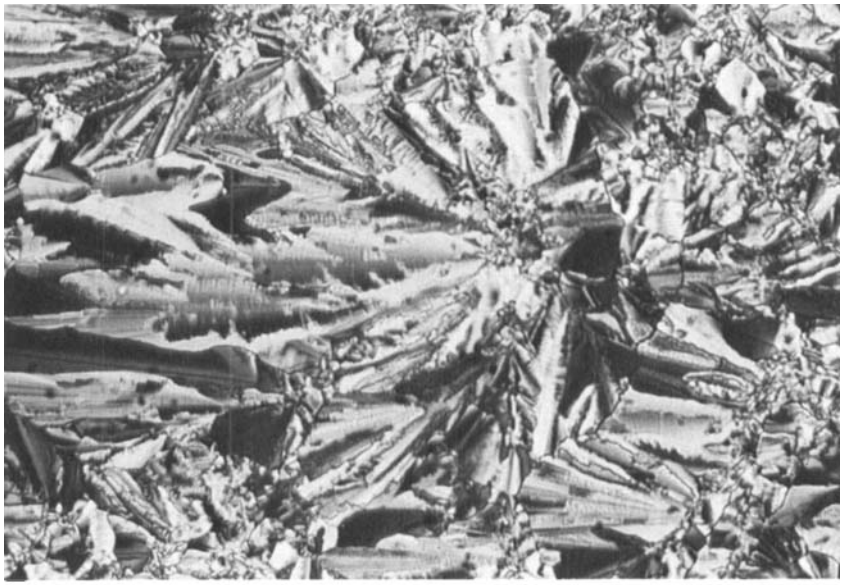

(a)

(b)

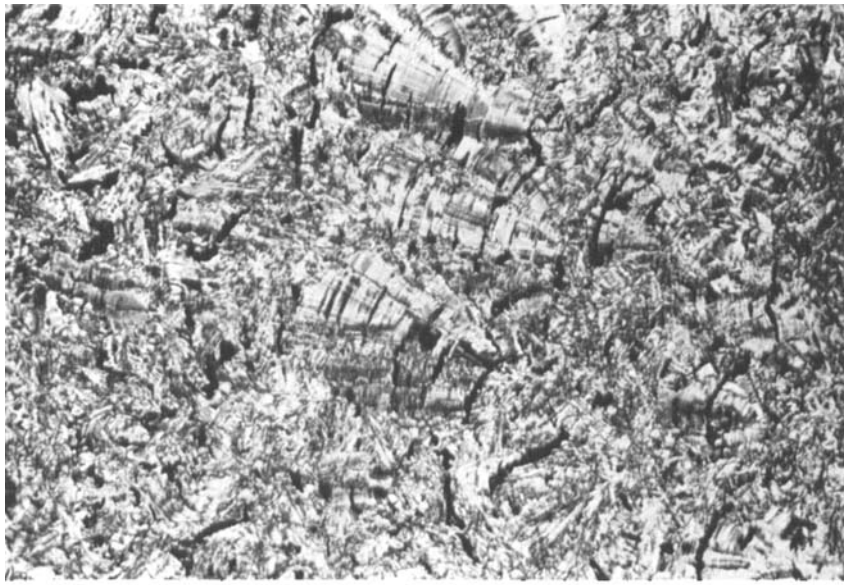

(c)

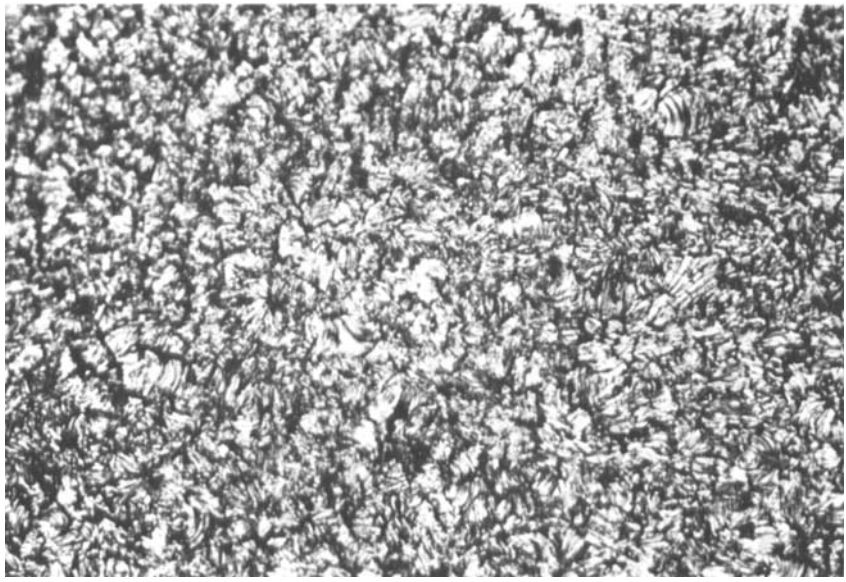

(d)

FIGURE 5 Optical textures of the columnar mesophase (a and b), Phase I (c) and Phase II (d) of $C_6(OCOC_7H_{15})_6$. Magnification 100×.

normal heat capacity of the mesophase the experimental value at 355.688 K was used. As seen in Figure 1, the solid-to-solid phase transition brings about a heat capacity jump as large as 738 J K^{-1} mol^{-1}. This discontinuity may arise from a drastic change in crystal structure and the excitation of molecular motions for the paraffinic moieties, as have been revealed from the infrared absorption spectra. On the other hand, the normal heat capacity is lowered by 124 J K^{-1} mol^{-1} on going from Phase I to the mesophase, while it is raised by 175 J K^{-1} mol^{-1} at the clearing point.

The enthalpy and entropy of the phase transitions were determined as being the excess contributions beyond these normal heat capacities. For these calculations, the results of the calorimetric enthalpy measurements across the respective phase transitions were also taken into account. The numerical data concerning the thermodynamic quantities due to the phase transitions are summarized in Table III. Figure 6 represents the temperature dependence of the entropy acquisition due to the phase transitions. One of the remarkable features is that, although the present compound exhibits only a single phase transition in the solid state, its entropy acquisition (ΔS = 164.01 J K^{-1} mol^{-1}) is quite large compared with the melting entropy of 129.81 J K^{-1} mol^{-1}. Along with the case of $C_6(OCOC_6H_{13})_6$,[16] the present study also indicates that solid polymorphism accompanied by a large amount of transition entropy is one of the necessary conditions for the appearance of the columnar mesophase. On the other hand, the melting entropy itself is not too large since it is only 2.4-fold as much as the transition entropy at the clearing point.

In the case of $C_6(OCOC_5H_{11})_6$, the successive phase transitions were well interpreted in terms of the conformational melting of the paraffinic chains progressing from the periphery of a molecule into its inside each time a phase transition takes place.[13] If this model could directly be applied for the present case, the cumulative entropy should amount to 410 J K^{-1} mol^{-1}; about 124 J K^{-1} mol^{-1} (the entropy gain per twelve methylene groups[13]) larger than the sum of transition entropy for $C_6(OCOC_5H_{11})_6$. But this is not the case. However, if the standard entropies of the present homologous series are compared, this puzzle seems to be easily solved. In Figure 7 we plotted the standard molar

TABLE III

Enthalpy and entropy of phase transitions in $C_6(OCOC_7H_{15})_6$

Transition	T_c/K	ΔH/kJ mol^{-1}	ΔS/J K^{-1} mol^{-1}
Phase II → Phase I	301.89	48.96	164.01
Phase I → Mesophase	355.10	46.07	129.81
Mesophase → Isotropic Liquid	357.09	19.22	53.77
			total 347.59

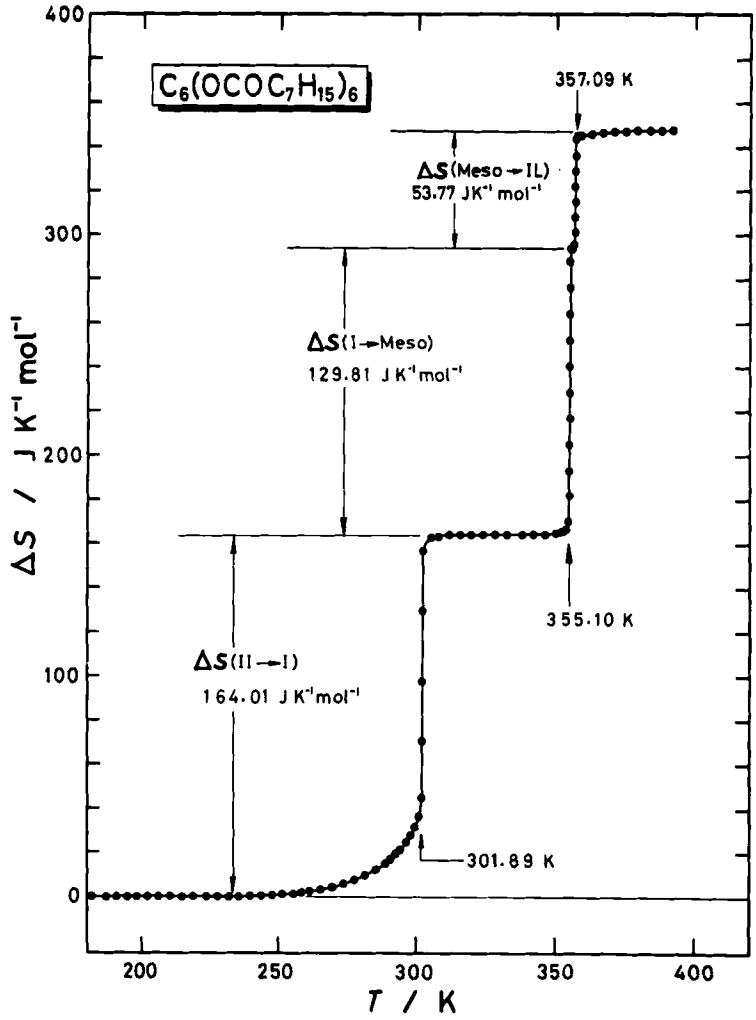

FIGURE 6 Temperature dependence of the entropy acquisition due to the phase transitions for $C_6(OCOC_7H_{15})_6$.

entropy for the homologous series, $C_6(OCOC_nH_{2n+1})_6$ (n = 5, 6 and 7), as a function of temperature. For convenience, the entropy has been divided by temperature. Although the cumulative transition entropies are irregular among the three homologous series, the standard entropy is increased regularly with the carbon number, n, of the paraffinic chain in the isotropic liquid phase, in which the molecular conformations are fully disordered. An essential difference between the discotic (n = 6 and 7) and non-discotic (n = 5) mesogens seems to become conspicuous at low temperatures below, say 250

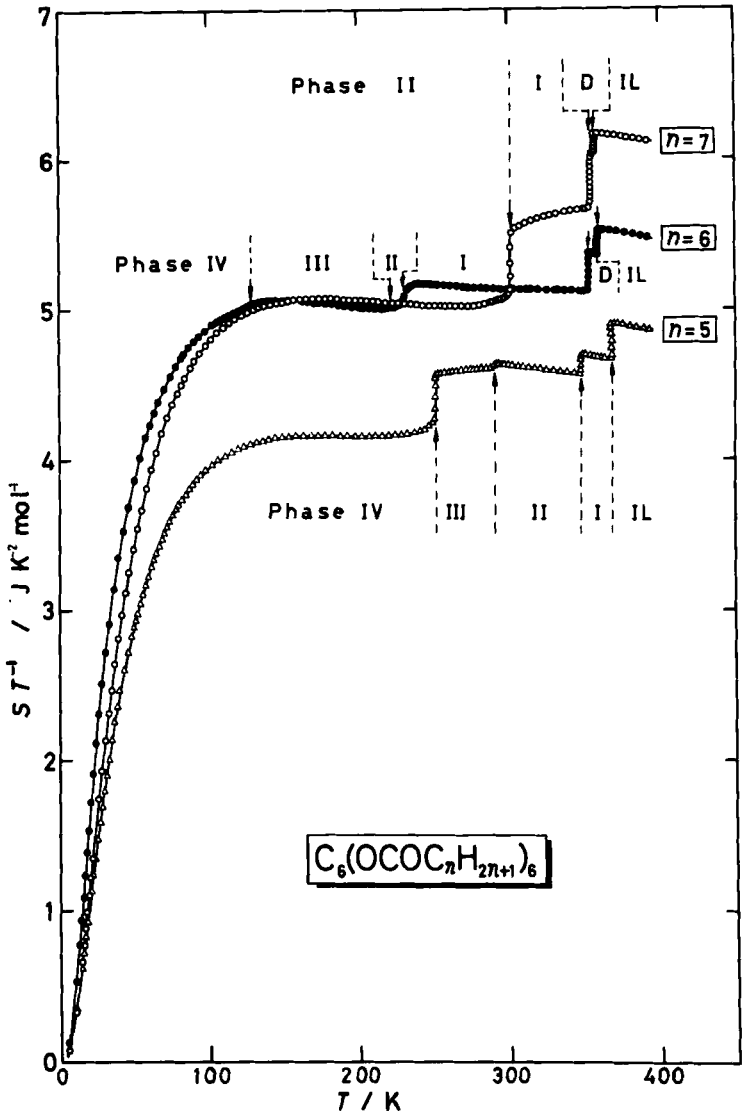

FIGURE 7 Temperature dependence of the standard molar entropy for $C_6(OCOC_nH_{2n+1})_6$ ($n = 5, 6, 7$). For convenience, the entropy is divided by temperature. "D" and "IL" indicate the columnar mesophase and isotropic liquid phase, respectively.

K. Namely, the discotic mesogens have already acquired considerable amount of the conformational entropy at low temperatures without accompanying dominant solid-to-solid phase transitions.

The S/T against T diagram (Figure 7) clearly shows that the columnar mesophase is a phenomenon appearing as one stage of the successive phase transi-

tion due to the conformational meltings of the paraffinic moieties. Moreover, in the sense that the solid polymorphism plays an important role for the appearance of a columnar mesophase, the analogy of the columnar mesophase to plastic crystal should be emphasized. Many workers have an image that plastic crystal consists of three-dimensional globular molecules whereas discotic mesogen has two-dimensional planar molecular structure. However, this is not necessarily correct because polycyclic aromatics having no flexible paraffinic chains such as coronene, ovalene, decacyclene etc., which can be regarded as two-dimensional molecules in a true sense, exhibit neither columnar mesophase nor dominant solid polymorphism.[24] In contrary to this, all the discotic mesogens hitherto known have flexible moieties bonded to a planar central core. As revealed from the calorimetric and infrared studies, the conformations of the paraffinic chains are highly disordered in the mesophase. In other words, the dynamic structure of a disc-like molecule is not so planar but even globular in the mesophase.

In connection with the progressive melting of paraffinic chains, it is of some interest to note that ionic quaternary ammonium compounds are known to exhibit solid polymorphism accompanied by a large amount of transition entropy though they do not bring about any mesophases.[25-27] The solid-to-solid transitions have been mainly attributed to a kink-block type melting[28] within the paraffinic moieties of the quaternary ammonium cation.

We have measured the heat capacities and recorded the infrared spectra of two enantiotropic discotic mesogens as well as their precursor among the benzene-hexa-*n*-alkanoates reported by Chandrasekhar *et al.*,[1,2] and found some characteristic features of the columnar mesophase from a thermodynamic point of view. Unfortunately, however, the temperature intervals in which the columnar mesophase persists stably are extremely narrow ($\Delta T/\mathrm{K} = 1.99 \sim 5.49$). In this regard, similar study on the discotic mesogens having triphenylene core[29] seems to be more appropriate for elucidation of thermodynamic properties of the columnar mesophase itself since their mesophase ranges are much wider ($\Delta T/\mathrm{K} = 11 \sim 63$).

Acknowledgments

The authors acknowledge Itoh Science Foundation for supplying them a polarizing microscope equipped with a heating stage. The infrared spectra were recorded by Messrs. S. Ishikawa and T. Yamamoto, to whom thanks are due.

References

1. S. Chandrasekhar, B. K. Sadashiva and K. A. Suresh, *Pramana*, **9**, 471 (1977).
2. S. Chandrasekhar, B. K. Sadashiva, K. A. Suresh, N. V. Madhusudana, S. Kumar, R. Shashidhar and G. Venkatesh, *J. Phys.* (*Paris*), **40**, C3-120 (1979).
3. S. Chandrasekhar, *Mol. Cryst. Liq. Cryst.*, **63**, 171 (1981).
4. A. M. Levelut, *J. Phys.* (*Paris*), **40**, L-81 (1979).

5. A. M. Levelut, *Proceedings of the International Liquid Crystals Conference,* Bangalore, December 1979, ed. S. Chandrasekhar, p. 21, Heyden, London (1980).
6. F. C. Frank and S. Chandrasekhar, *J. Phys. (Paris)*, **41,** 1285 (1980).
7. J. Billard, J. C. Dubois, C. Vaucher and A. M. Levelut, *Mol. Cryst. Liq. Cryst.*, **66,** 115 (1981).
8. N. H. Tinh, H. Gasparoux and C. Destrade, *Mol. Cryst. Liq. Cryst.*, **68,** 101 (1981).
9. C. Destrade, N. H. Tinh, H. Gasparoux, J. Malthete and A. M. Levelut, *Mol. Cryst. Liq. Cryst.*, **71,** 111 (1981).
10. J. Billard, J. C. Dubois, N. H. Tinh and A. Zann, *Nouv. J. Chim.*, **2,** 535 (1978).
11. W. Helfrich, *Proceedings of the International Liquid Crystals Conference,* Bangalore, December 1979, ed. S. Chandrasekhar, p. 7, Heyden, London (1980).
12. W. Helfrich, *J. Phys. (Paris)*, **40,** C3–105 (1979).
13. M. Sorai, K. Tsuji, H. Suga and S. Seki, *Mol. Cryst. Liq. Cryst.*, **59,** 33 (1980).
14. M. Sorai, K. Tsuji, H. Suga and S. Seki, *Proceedings of the International Liquid Crystals Conference,* Bangalore, December 1979, ed. S. Chandrasekhar, p. 41, Heyden, London (1980).
15. M. Sorai, K. Tsuji, H. Suga and S. Seki, the 8th International Liquid Crystal Conference, Kyoto, July 1980.
16. M. Sorai and H. Suga, *Mol. Cryst. Liq. Cryst.*, **73,** 47 (1981).
17. F. A. Hoglan and E. Bartow, *J. Am. Chem. Soc.*, **62,** 2397 (1940).
18. I. E. Neifert and E. Bartow, *J. Am. Chem. Soc.*, **65,** 1770 (1943).
19. *Organic Syntheses,* Coll. Vol. 5, p. 595 and p. 1011 (1973).
20. M. Yoshikawa, M. Sorai, H. Suga and S. Seki, to be published.
21. K. Tsuji, M. Sorai, H. Suga and S. Seki, *Mol. Cryst. Liq. Cryst.*, **55,** 71 (1979).
22. K. S. Pitzer and W. D. Gwinn, *J. Chem. Phys.*, **10,** 428 (1942).
23. M. Sorai and S. Seki, *J. Phys. Soc. Japan,* **32,** 382 (1972).
24. G. W. Smith, *Mol. Cryst. Liq. Cryst.*, **64,** L–15 (1980).
25. T. G. Coker, B. Wunderlich and G. J. Janz, *Trans. Faraday Soc.*, **65,** 3361 (1969).
26. T. G. Coker, J. Ambrose and G. J. Janz, *J. Am. Chem. Soc.*, **92,** 5293 (1970).
27. J. T. S. Andrews and J. E. Gordon, *J. Chem. Soc. Faraday Trans. I,* **69,** 546 (1973).
28. S. Blasenbrey and W. Pechhold, *Rheologica Acta,* **6,** 174 (1967).
29. C. Destrade, M. C. Mondon and J. Malthete, *J. Phys. (Paris)*, **40,** C3–17 (1979).